Pergamon

Int. J. Solids Structures Vol. 33, No. 10, pp. 1409–1424, 1996
Copyright © 1996 Elsevier Science Ltd
Printed in Great Britain. All rights reserved
0020–7683/96 $15.00 + .00

0020–7683(95)00108–5

DYNAMIC STABILITY OF A TAPERED CANTILEVER BEAM ON AN ELASTIC FOUNDATION SUBJECTED TO A FOLLOWER FORCE

H. P. LEE
Department of Mechanical and Production Engineering, National University of Singapore, 10 Kent Ridge Crescent, Singapore 0511

(*Received* 11 *November* 1994; *in revised form* 5 *April* 1995)

Abstract—The equation of motion in matrix form of a tapered cantilever Euler beam subjected to a follower force at the free end is formulated based on the Lagrangian approach and the assumed mode method. The beam is resting on a Winkler-type elastic foundation. The effects of the presence of viscous damping in the foundation, which makes the foundation viscoelastic, and the presence of internal damping in the beam on the critical flutter loads are examined separately to evaluate their relative importance. As expected, internal damping of the beam tends to drastically reduce the critical flutter loads for a beam of uniform cross-section. For tapered beams, the effects are however dependent on the taper ratio of the beam as well as the modulus of the elastic foundation. The critical flutter loads of both tapered beams and beams of uniform cross-section are found to be unaffected by the presence of viscous damping in the elastic foundation. The effect of varying the modulus of the elastic foundation on the critical flutter loads is also discussed in the paper.

1. INTRODUCTION

The dynamic stability of a rod subjected to follower forces has been studied extensively since the early works by Bolotin (1964, 1965) and Ziegler (1968). The unstable behavior may occur in the form of divergence or flutter as the follower forces are nonconservative forces. A detailed discussion of this subject and a comprehensive list of references can be found in the book by Leipholz (1980). This problem is often analyzed using numerical methods such as the finite difference method [for example, Leipholz (1980); Guran and Rimrott (1989); Nageswara Rao and Venkateswara Rao (1987, 1988, 1990); the Ritz method (Levinson, 1966); the finite element method (Ryu and Sugiyama, 1994) and many other forms of discretization methods (De Rosa and Franciosi, 1990; Lee *et al.*, 1992)].

The presence of a small amount of damping has been recognized in the early studies [for example, Bolotin and Zhinzher (1969); Herrmann and Jong (1965, 1966); Nemat-Nasser (1967)] to have a strong influence on the dynamic stability of nonconservative systems. In all the reported cases, the critical flutter loads for systems involving damping are found to be smaller than the corresponding critical flutter loads obtained without damping, a phenomenon described as the "destabilizing effect" of damping in a number of studies [for example, Herrmann and Jong (1965); Leipholz (1980)]. Leipholz (1980) asserted that the effects of internal damping, or Voigt–Kelvin damping, may be neglected for systems with the smallest critical load associated with the divergence-type instability, but must be taken into consideration for systems which become unstable in the form of flutter.

The dynamic stability of a beam resting on an elastic foundation was first examined by Smith and Herrmann (1972). The critical flutter loads for a beam of uniform cross-section were found to be independent of the foundation modulus which characterizes the Winkler-type elastic foundation. A detailed study on the stability of a beam of elastic foundation subjected to conservative and nonconservative forces was reported by Sundararajan (1974). The effects of an elastic foundation with variable foundation modulus distribution were examined by Hauger and Vetter (1976). The dynamic stability of a tapered beam resting on an elastic foundation was examined by Venkateswara Rao and Kanaka Raju (1982) using the finite element method. The critical flutter loads of tapered beams

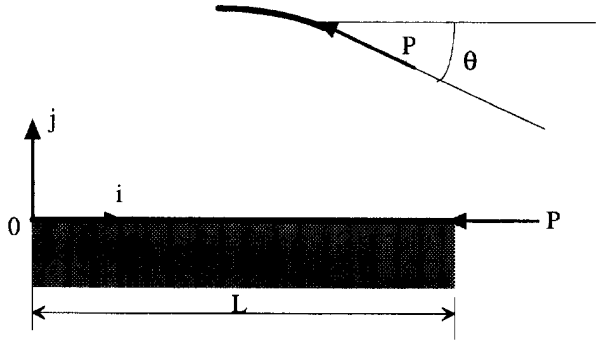

Fig. 1. A cantilever rod on an elastic foundation subjected to a follower force.

were reported to be relatively unaffected by the variation of the dimensionless modulus of the elastic foundation. However, the range of the variation of the dimensionless modulus of elastic foundation from 0 to 100 reported in their work was relatively small. Lee and Yang (1994), using the transfer matrix method, reported a large variation of the critical flutter loads for a tapered beam resting on an elastic foundation with a large variation in the foundation modulus. However, the effect of damping was not included in all of these studies. The present model is related to the dynamics of a rocket or an aeroplane wing subjected to follower forces caused by rocket thrust or jet-engines.

In the present paper, the equation of motion in matrix form of a clamped-free tapered Euler beam subjected to a follower force applied at the free end of the rod is formulated based on Lagrangian approach and the assumed mode method. The beam is resting on a Winkler-type elastic foundation of uniform modulus. The nonconservative nature of the system can be easily identified in the present matrix formulation by the presence of a non-symmetric matrix in the equation of motion. The objective is to investigate how the presence of a small amount of internal damping in the beam and viscous damping in the elastic foundation will affect the critical follower force of a tapered beam.

2. THEORY AND FORMULATIONS

Figure 1 shows a clamped-free rod of length L of non-uniform cross-section, Young's modulus E, central principle second moment of area I, cross-sectional area A, and mass m per unit length. As the beam is assumed to be tapered, I, A and m are dependent on the location along the beam. The rod is subjected to a follower force of magnitude P applied at the free end of the rod. The deflection of the rod is assumed to be small for the behavior to be governed by Euler's beam theory. A set of right-handed mutually perpendicular unit vectors, **i** and **j**, is assumed to be fixed in the undeformed rod with the **i** unit vector parallel to the undeformed neutral axis of the rod. The deflection for a point on the rod is denoted by $w(x, t)$ with t denoting the time and x the distance along the beam measured from the clamped end of the beam.

For small deflection, the slope at the free end of the rod, θ, indicated in Fig. 1 can be approximated by $\partial w/\partial x$ evaluated at $x = \mathrm{L}$. Moreover, $\cos\theta \approx 1$ and $\sin\theta \approx \theta$. The axial component of the follower force in the **i** direction, parallel to the neutral axis of the undeformed rod, is equal to $P\cos\theta \approx P$ for small deflection, neglecting quantity of the order of (w^2) and smaller. The transverse component in the **j** direction, normal to the neutral axis of the undeformed rod, is given by $P\sin(\partial w/\partial x) \approx P(\partial w/\partial x)$ evaluated at $x = L$. Therefore, the work done by the follower force can be divided into two parts. The potential energy due to the axial component of the follower force is

$$V_a = -\frac{1}{2}\int_0^L P\left(\frac{\partial w}{\partial x}\right)^2 \mathrm{d}x. \tag{1}$$

The transverse component of the follower force is a nonconservative force and no potential energy can be defined for this force component. The virtual work, δW, of this transverse component of the follower force can be expressed as

$$\delta W = -P\frac{\partial w}{\partial x}(x = L, t)\delta w(x = L, t) \tag{2}$$

where $\delta w(x = L, t)$ is the virtual transverse displacement at the free end of the rod where the follower force is applied.

The elastic strain energy of the rod due to bending is

$$V_\varepsilon = \frac{1}{2}\int_0^L EI\left(\frac{\partial^2 w}{\partial x^2}\right)^2 \mathrm{d}x. \tag{3}$$

The elastic strain energy due to the Winkler-type elastic foundation of modulus k per unit length is

$$V_k = \tfrac{1}{2}k\int_0^L w^2 \,\mathrm{d}x. \tag{4}$$

With $\dot{w}$ defined as $\dfrac{\mathrm{d}w}{\mathrm{d}t}$, the total kinetic energy T of the rod is

$$T = \frac{1}{2}\int_0^L m\dot{w}^2 \,\mathrm{d}x. \tag{5}$$

For simplicity, the following dimensionless quantities are introduced

$$\tau = t\sqrt{\frac{EI}{m_0 L^4}}, \quad \xi = \frac{x}{L}, \quad \bar{P} = \frac{PL^2}{EI_0}, \quad \bar{k} = \frac{kL^3}{EI_0}. \tag{6}$$

The quantities m_0 and I_0 denote respectively the values of m and I at the clamped end of the beam with $\xi = 0$. The tapered beam is assumed to be a beam of rectangular cross-section with linearly varied height and width with α_b and α_h denoting respectively the taper ratios of the width and the height of the cross-section. The quantities m and I therefore vary as

$$I(\xi) = I_0(1-\alpha_b\xi)(1-\alpha_h\xi)^3 \tag{7}$$

$$m(\xi) = m_0(1-\alpha_b\xi)(1-\alpha_h\xi). \tag{8}$$

The dimensionless w is given by

$$\bar{w} = \frac{w}{L} = \sum_{i=1}^{n} \bar{q}_i(\tau)\phi_i(\xi). \tag{9}$$

The normalized beam functions for a beam clamped at $\xi = 0$ and free at $\xi = 1$ are

$$\phi_i(\xi) = \sin\beta\xi - \sinh\beta\xi - \gamma(\cos\beta\xi - \cosh\beta\xi) \tag{10}$$

where β are the eigenvalues that satisfy the characteristic equation for the beam vibration with one end clamped and the other end free and

$$\gamma = \frac{\sin\beta + \sinh\beta}{\cos\beta + \cosh\beta}. \tag{11}$$

The resulting dimensionless equation of motion for a rod without damping is

$$\bar{\mathbf{M}}\ddot{\bar{\mathbf{q}}} + (\bar{\mathbf{K}} + \bar{k}\bar{\mathbf{H}} - \bar{P}(\bar{\mathbf{A}} - \bar{\mathbf{D}}))\bar{\mathbf{q}} = \mathbf{0}. \tag{12}$$

The matrices in the above equation are defined as

$$(\bar{\mathbf{H}})_{ij} = \int_0^1 \phi_i \phi_j \, \mathrm{d}\xi \tag{13}$$

$$(\bar{\mathbf{M}})_{ij} = \int_0^1 (1 - \alpha_b \xi)(1 - \alpha_h \xi)\phi_i \phi_j \, \mathrm{d}\xi \tag{14}$$

$$(\bar{\mathbf{K}})_{ij} = \int_0^1 (1 - \alpha_b \xi)(1 - \alpha_h \xi)^3 \phi_i'' \phi_j'' \mathrm{d}\xi \tag{15}$$

$$(\bar{\mathbf{A}})_{ij} = \int_0^s \phi_i' \phi_j' \, \mathrm{d}\xi \tag{16}$$

$$(\bar{\mathbf{D}})_{ij} = \phi_i(\xi = 1)\phi_j'(\xi = 1). \tag{17}$$

The matrix $\bar{\mathbf{H}}$ is an identity matrix $\mathbf{I}$ due to the orthogonality of the assumed functions. The functions ϕ_i' and ϕ_i'' denote the first and second derivatives of ϕ_i with respect to ξ. The vectors $\bar{\mathbf{q}}$ and $\dot{\bar{\mathbf{q}}}$ are $n \times 1$ column vectors. All the matrices except $\bar{D}$ are symmetric matrices. The nonsymmetric matrix $\bar{\mathbf{D}}$ in the above equation of motion makes the system non-conservative.

In the presence of internal damping or Voigt–Kelvin damping, an additional term $\eta\bar{\mathbf{K}}\dot{\bar{\mathbf{q}}}$ (Leipholz, 1980) can be included in the equation of motion where η is the damping factor. The resulting equation of motion for a rod with internal damping is

$$\bar{\mathbf{M}}\ddot{\bar{\mathbf{q}}} + \eta\bar{\mathbf{K}}\dot{\bar{\mathbf{q}}} + (\bar{\mathbf{K}} + \bar{k}\bar{\mathbf{H}} - \bar{P}(\bar{\mathbf{A}} - \bar{\mathbf{D}}))\bar{\mathbf{q}} = \mathbf{0}. \tag{18}$$

If the elastic foundation is viscoelastic with dimensionless viscous damping coefficient c, instead of the term $\eta\bar{\mathbf{K}}\dot{\bar{\mathbf{q}}}$, the term to be added in the equation of motion is $c\bar{\mathbf{H}}\dot{\bar{\mathbf{q}}}$. The resulting equation of motion for a rod resting on a viscoelastic foundation is therefore given by

$$\bar{\mathbf{M}}\ddot{\bar{\mathbf{q}}} + c\bar{\mathbf{H}}\dot{\bar{\mathbf{q}}} + (\bar{K} + \bar{k}\bar{\mathbf{H}} - \bar{P}(\bar{\mathbf{A}} - \bar{\mathbf{D}}))\bar{\mathbf{q}} = \mathbf{0}. \tag{19}$$

The equations of motion can be rearranged in the following form

$$\dot{\mathbf{z}} = \mathbf{B}\mathbf{z} \tag{20}$$

with

$$\mathbf{z} = \begin{bmatrix} \dot{\bar{\mathbf{q}}} \\ \bar{\mathbf{q}} \end{bmatrix} \tag{21}$$

$$\mathbf{B} = \begin{bmatrix} -\eta\bar{\mathbf{K}} & -(\bar{\mathbf{K}} + \bar{k}\bar{\mathbf{H}} - \bar{P}(\bar{\mathbf{A}} - \bar{\mathbf{D}})) \\ \mathbf{I} & \mathbf{0} \end{bmatrix} \quad \text{for internal damping} \tag{22}$$

$$\mathbf{B} = \begin{bmatrix} -c\bar{\mathbf{H}} & -(\bar{\mathbf{K}} + \bar{k}\bar{\mathbf{H}} - \bar{P}(\bar{\mathbf{A}} - \bar{\mathbf{D}})) \\ \mathbf{I} & \mathbf{0} \end{bmatrix} \quad \text{for viscous damping.} \tag{23}$$

The corresponding characteristic equation is given by

$$\det |\mathbf{B} - \omega \mathbf{I}| = 0 \tag{24}$$

where ω are the complex eigenvalues of the real asymmetric matrix $\mathbf{B}$. The stability of the rod is determined by the sign of the real part of ω. A positive real part indicates that the motion is unstable.

It should be pointed out that as discussed in Lee (1994), the assumed functions for w for the present assumed mode method need not satisfy the natural boundary conditions at the free end of the rod. These natural boundary conditions at the free end should be (Kounadis, 1983)

$$\frac{\partial^2 w}{\partial x^2} = 0 \tag{25}$$

$$\frac{\partial^3 w}{\partial x^3} + \frac{P}{EI}\frac{\partial w}{\partial x} = 0. \tag{26}$$

The second boundary condition regarding the transverse shear force was erroneously written as $\partial^3 w/\partial x^3 = 0$ in a number of reported works [for example, Smith and Herrmann (1972); Venkateswara Rao and Kanaka Raju (1982); Elishakoff and Lottati (1988), Guran and Rimrott (1989)].

3. NUMERICAL RESULTS AND DISCUSSION

The convergence of the critical loads in terms of the number of terms for $\bar{w}$ is first examined. Although the convergence is not uniform, as pointed out by Leipholz (1980) for Galerkin's method, it is found that the first critical flutter loads for all the cases under consideration are almost converged for $n = 5$. The computations of the eigenvalues are relatively straightforward and fast with the use of PCMatlab on a personal computer. The only time consuming part of the computation is the derivation of the matrices $\bar{\mathbf{M}}$ and $\bar{\mathbf{K}}$ by numerical integrations. The matrices $\bar{\mathbf{M}}$ and $\bar{\mathbf{K}}$ are first expanded into components pre-multiplied by factors involving α_b and α_h before performing the numerical integration for each component. The matrices $\bar{\mathbf{M}}$ and $\bar{\mathbf{K}}$ for various combinations of α_b and α_h can then be computed easily by simple additions and multiplications without further numerical integrations.

The load–frequency diagrams for various combinations of damping and modulus of elastic foundation for a beam of uniform cross-section are shown in Fig. 2. As the eigenvalues are in general complex in the presence of damping, the load–frequency curves are presented with the horizontal axis in terms of the product terms of $\omega\omega^*$ which is always a positive real value. The divergence instability can be easily identified in these diagrams by the intersection of the curve and the vertical axis with $\omega\omega^* = 0$. If the imaginary part of ω as presented in all the other reported studies is used in place of $\omega\omega^*$ in these diagrams, the divergence behavior could not be identified without also examining the real part of ω for general cases in the presence of damping. In the absence of damping, the critical flutter load can be determined easily from the apex of the dome-shape structures, which corresponds to the coalescence of the eigenvalues at that point. In the presence of damping, the critical flutter load can be determined by examining the real part of the eigenvalues.

There are five sets of curves presented in each subplot of Fig. 2. The curve appearing on the extreme left side of each subplot is the load–frequency diagram for $\bar{k} = 1000$. With

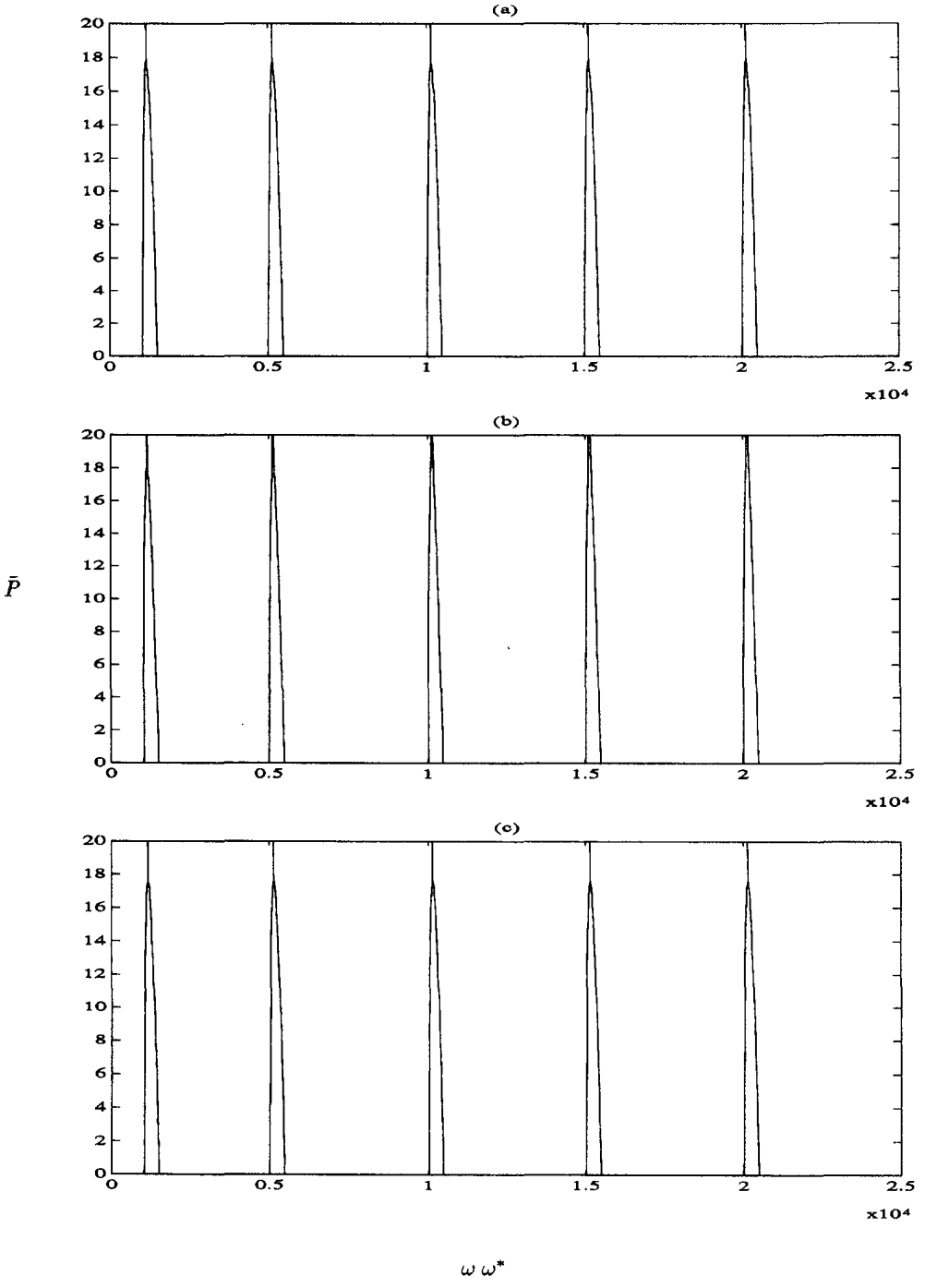

Fig. 2. The load–frequency curves for a cantilever rod of uniform cross-section subjected to a follower force on an elastic foundation with $\bar{k}$ varying between 1000 and 20,000. (a) No damping; (b) internal damping with $\eta = 0.001$; (c) viscous damping with $c = 0.1$.

increased modulus of the elastic foundation, the curves are found to be shifted to the right with increased magnitude of ω. The remaining four sets of curves presented in each subplot are for $\bar{k} = 5000$, 10,000, 15,000 and 20,000 respectively. For a beam of uniform cross-section without damping with the numerical results presented in Fig. 2(a), it can be seen that the critical flutter load, corresponding to the apex of the dome-shape structure for each curve, is insensitive to variation in the modulus of the elastic foundation. This finding

is in agreement with the reported findings by Smith and Herrmann (1972) and Lee and Yang (1994). The load–frequency diagrams for a beam of uniform cross-section with internal damping in the beam and viscous damping in the elastic foundation are shown respectively in Figs 2(b,c). It can be seen from Fig. 2(b) that the dome-shape structure disappears with the presence of small amount of internal damping with $\eta = 0.001$. The critical flutter load cannot be determined from the load–frequency diagram. However, for a beam resting on a viscoelastic foundation with $c = 0.1$, the load–frequency diagrams remain almost unchanged compared with the curves presented in Fig. 2(a). The real parts of the eigenvalues for the curves shown in Fig. 2 are presented in Fig. 3. It can be seen from Fig. 3(a) that the curves are almost coincident. The real part of the eigenvalues become positive at the critical flutter load which appears to be insensitive to the variation in the modulus of the elastic foundation, confirming the numerical results shown in Fig. 2(a). The critical flutter load also remains independent of the variation of the modulus of elastic foundation for a beam with viscous damping [see Fig. 3(c)]. Moreover, the critical flutter load for a beam resting on a viscoelastic foundation with $c = 0.1$ is almost the same as the critical flutter load for a beam resting on an elastic foundation without damping. Cases for other reasonable values of c for the range between 0 and 0.2 have also been examined and the finding remains valid. However, in the presence of small amounts of internal damping with $\eta = 0.001$, the curves that appear in Fig. 3(b) are found to begin from the negative region, not shown in the diagram, intersecting the vertical line and entering the positive region at a critical value of $\bar{P}$ very much smaller than the critical flutter load for the beam without damping. With increased amounts of internal damping (numerical results are not shown), the points of intersection of these curves with the vertical axis are found to remain almost unaffected by the increase in damping factor. The rapid growing of the real part of ω with increased value of $\bar{P}$ only begins when the real part of ω is positive, consistent with the reported finding by Bolotin and Zhinzher (1969). The presence of small amounts of damping has therefore resulted in a sharp reduction of the critical flutter load, a phenomenon known as the "destabilizing effect" of damping in a number of reported studies.

The load–frequency diagrams for a tapered beam with constant height ($\alpha_h = 0$) and uniformly tapered width are shown in Fig. 4 for the case without damping. Once again, the five sets of curves presented in each subplot are for $\bar{k} = 1000$, 5000, 10,000, 15,000 and 20,000 respectively with the extreme left curve corresponding to the case of $\bar{k} = 1000$. The taper ratio α_b for the curves presented in Figs 3(a,b,c) are respectively 0.05, 0.2 and 0.5. Unlike the numerical results for a beam with uniform cross-section, the critical flutter load for a tapered beam is found to be dependent on the modulus of the elastic foundation. In general, the critical flutter load is found to increase with increased modulus of the elastic foundation although the rate of increase is dependent on the taper ratio. For example, the rate of increase of the critical flutter load with increased $\bar{k}$ is relatively small for $\bar{k}$ smaller than 5000 and for $\bar{k}$ larger than 10,000 for the case shown in Fig. 4(a) with $\alpha_b = 0.05$. There is a sharp increase in the critical flutter load when $\bar{k}$ is varied from 5000 to 10,000, consistent with the numerical results presented by Lee and Yang (1994). The reported finding by Venkateswara Rao and Kanaka Raju (1982) that the critical flutter load is relatively insensitive to variation of $\bar{k}$ is mainly due to the narrow range of variation of $\bar{k}$ from 1 to 100 in their reported study. The real parts of ω for the curves shown in Fig. 4 are presented in Fig. 5. It can be seen that the real part becomes positive and increases rapidly when the follower force reaches the respective critical flutter load for each case.

The effect of the presence of a small amount of internal damping $\eta = 0.001$ on the cases shown in Fig. 4 is examined in Fig. 6. It can be seen from Fig. 6 that the presence of internal damping destroys the dome-shape structure in these load–frequency diagrams and makes the determination of the critical flutter loads impossible without examining the real part of the eigenvalues which are shown in Fig. 7. It can be seen from these diagrams that the effect of internal damping is dependent on both the taper ratio α_b and the modulus of elastic foundation $\bar{k}$. For the curves shown in Fig. 7(a) with $\alpha_b = 0.05$ and comparing with the corresponding curves shown in Fig. 5(a), the presence of internal damping is found to drastically reduce the critical flutter load only for the case of $\bar{k} = 1000$. The critical flutter loads for the remaining four cases with larger values of $\bar{k}$ remain relatively unaffected by

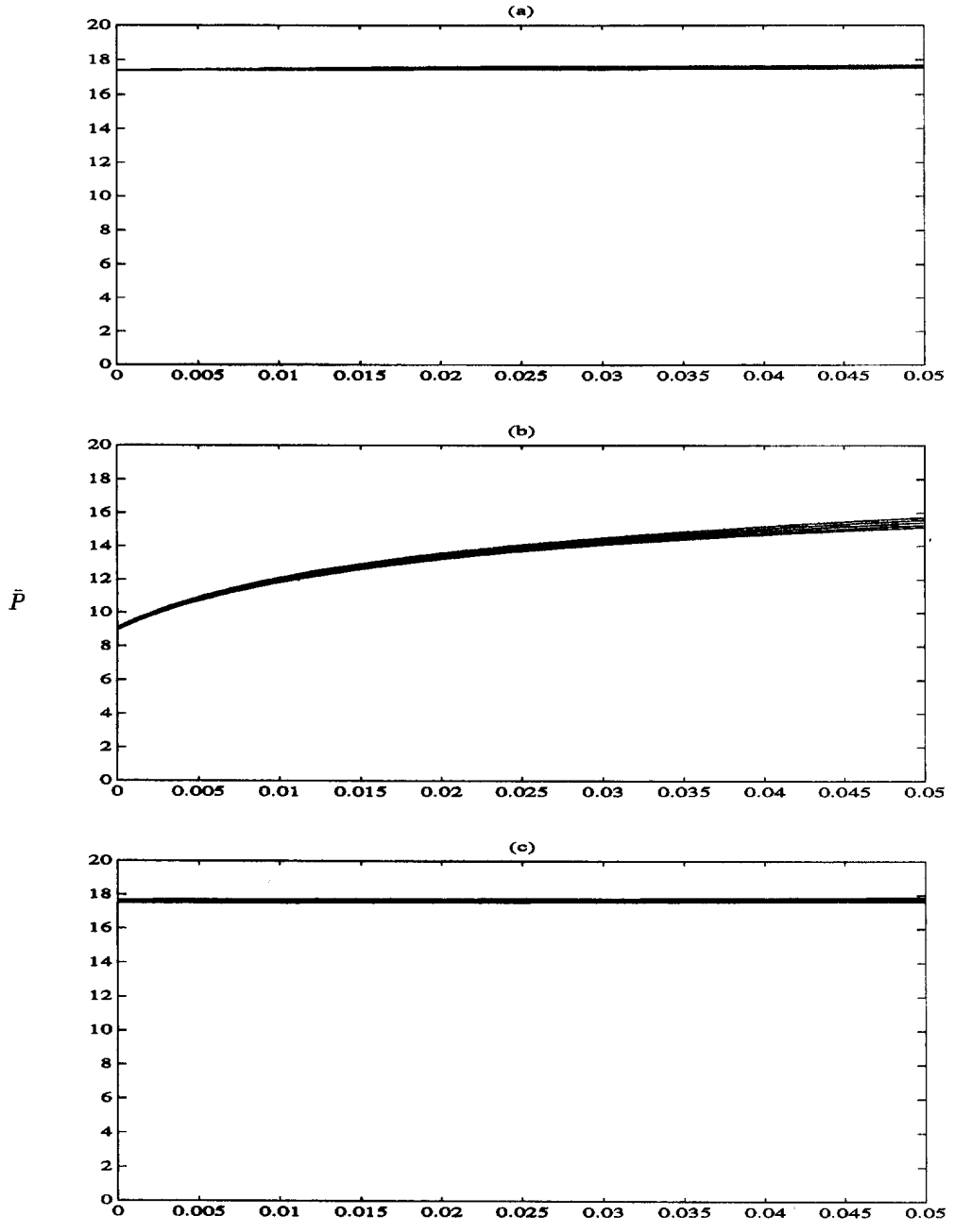

Fig. 3. The real part of ω for the load–frequency curves presented in Fig. 2. (a) No damping; (b) internal damping with $\eta = 0.001$; (c) viscous damping with $c = 0.1$.

the presence of internal damping. However, for the curves shown in Fig. 7(b) with $\alpha_b = 0.2$, the presence of internal damping does not affect the case of $\bar{k} = 1000$ but does reduce the critical flutter loads for the remaining four cases. For the curves shown in Fig. 7(c), the presence of internal damping does not affect the cases with $\bar{k} = 1000$ and 5000, but increases the critical flutter loads for the remaining three cases. It can therefore be concluded that

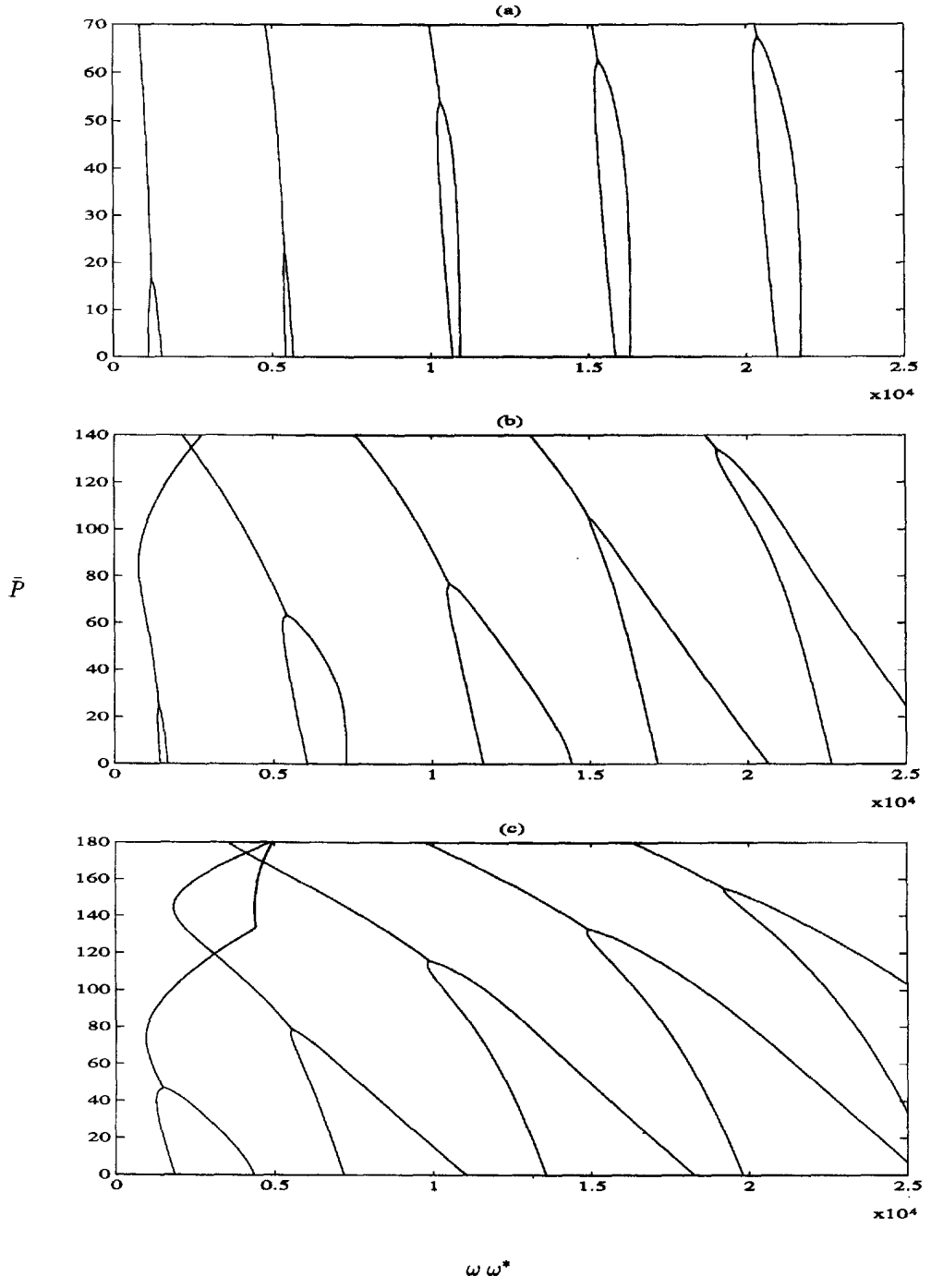

Fig. 4. The load–frequency curves for a tapered cantilever rod ($\alpha_b = 0$) subjected to a follower force on an elastic foundation with $\bar{k}$ varying between 1000 and 20,000. (a) $\alpha_b = 0.05$; (b) $\alpha_b = 0.2$; (c) $\alpha_b = 0.5$.

the effect of internal damping is dependent on both the taper ratio of the beam as well as the modulus of the elastic foundation.

The load frequency diagrams for a tapered beam with constant width ($\alpha_b = 0$) and uniformly tapered height are shown in Fig. 8 for the case without damping and in Fig. 9 for the case with the presence of small amount of internal damping. The curves presented

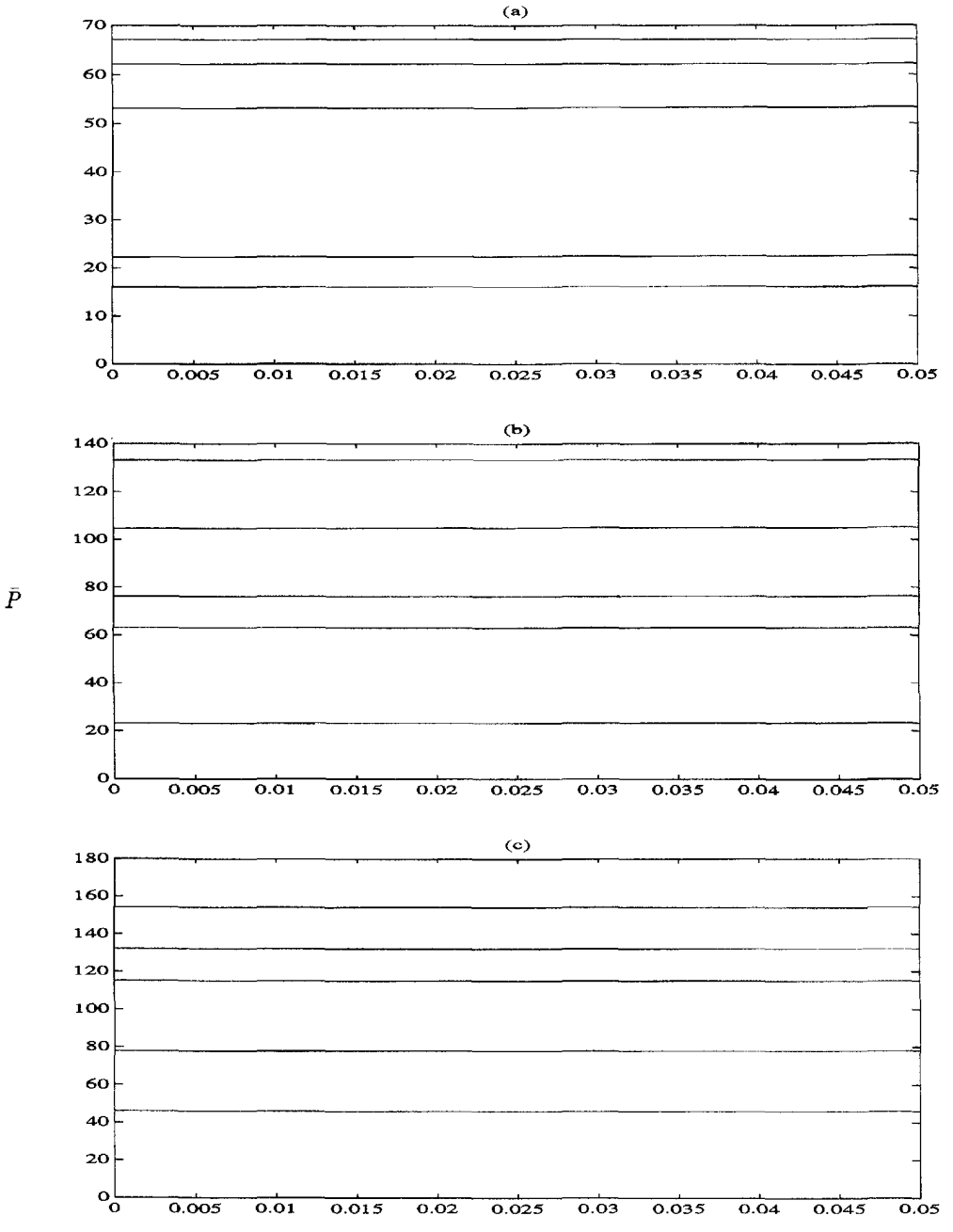

Fig. 5. The real part of ω for the load–frequency curves presented in Fig. 4. (a) $\alpha_b = 0.05$; (b) $\alpha_b = 0.2$; (c) $\alpha_b = 0.5$.

in Fig. 8 show that the critical flutter loads are in general larger with larger modulus of elastic foundation. The rate of increase with increased $\bar{k}$ is once again dependent on the taper ratio of the beam. The real parts of the curves shown in Fig. 9 are presented in Fig. 10 to determine the critical flutter loads for the case with the presence of internal damping. The effect of internal damping is once again dependent on the taper ratio as well as the

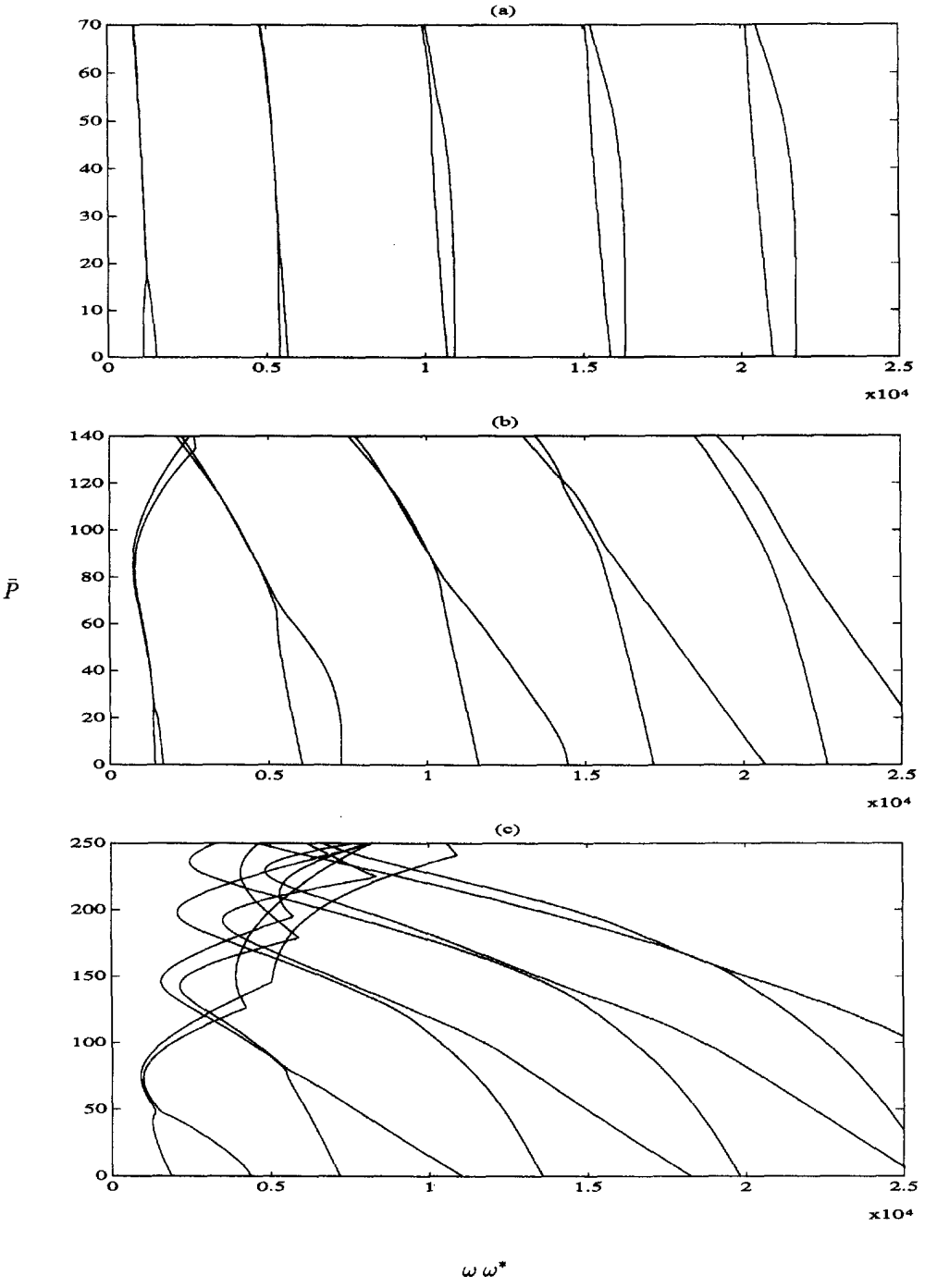

Fig. 6. The load–frequency curves for a tapered cantilever rod ($\alpha_h = 0$) subjected to a follower force on an elastic foundation with $\bar{k}$ varying between 1000 and 20,000. $\eta = 0.001$. (a) $\alpha_b = 0.05$; (b) $\alpha_b = 0.2$; (c) $\alpha_b = 0.5$.

modulus of elastic foundation. For the curves shown in Fig. 10(a) with $\alpha_h = 0.05$, the presence of internal damping is found to drastically reduce the critical flutter load only for the case of $\bar{k} = 1000$ [comparing with Fig. 8(a)]. The critical flutter loads for the remaining four cases with larger values of $\bar{k}$ remain relatively unaffected by the presence of internal damping. For the curves shown in Fig. 10(b) with $\alpha_h = 0.2$, the presence of internal

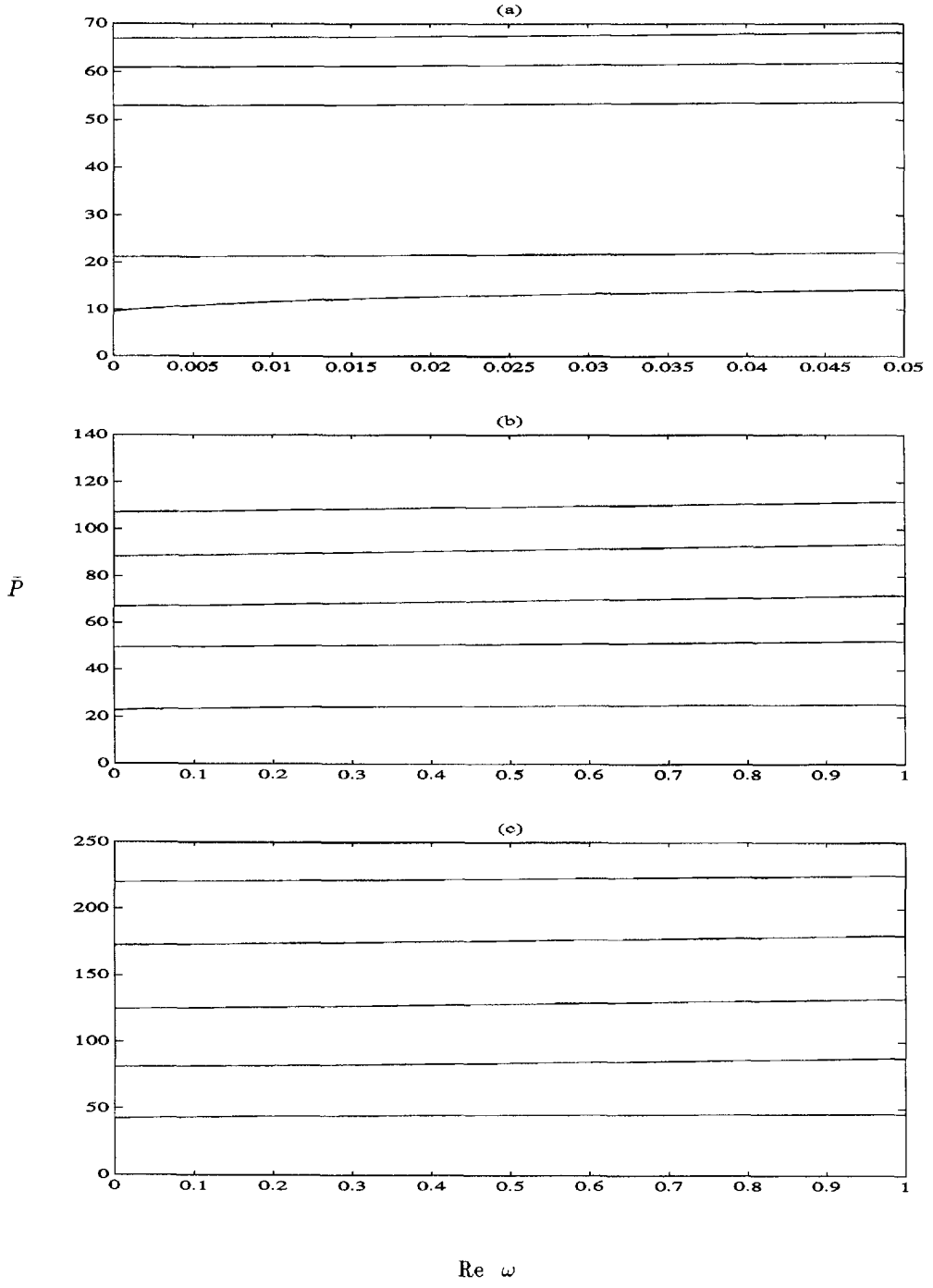

Fig. 7. The real part of ω for the load–frequency curves presented in Fig. 6. $\eta = 0.001$. (a) $\alpha_h = 0.05$; (b) $\alpha_h = 0.2$; (c) $\alpha_h = 0.5$.

damping does not affect the case of $\bar{k} = 1000$, 5000 and 10,000 but does increase the critical flutter loads for the remaining two cases. Similarly, for the curves shown in Fig. 10(c) with $\alpha_h = 0.5$, the presence of internal damping does not affect the case of $\bar{k} = 1000$, 5000, and 10,000 but does increase the critical flutter loads for the remaining two cases.

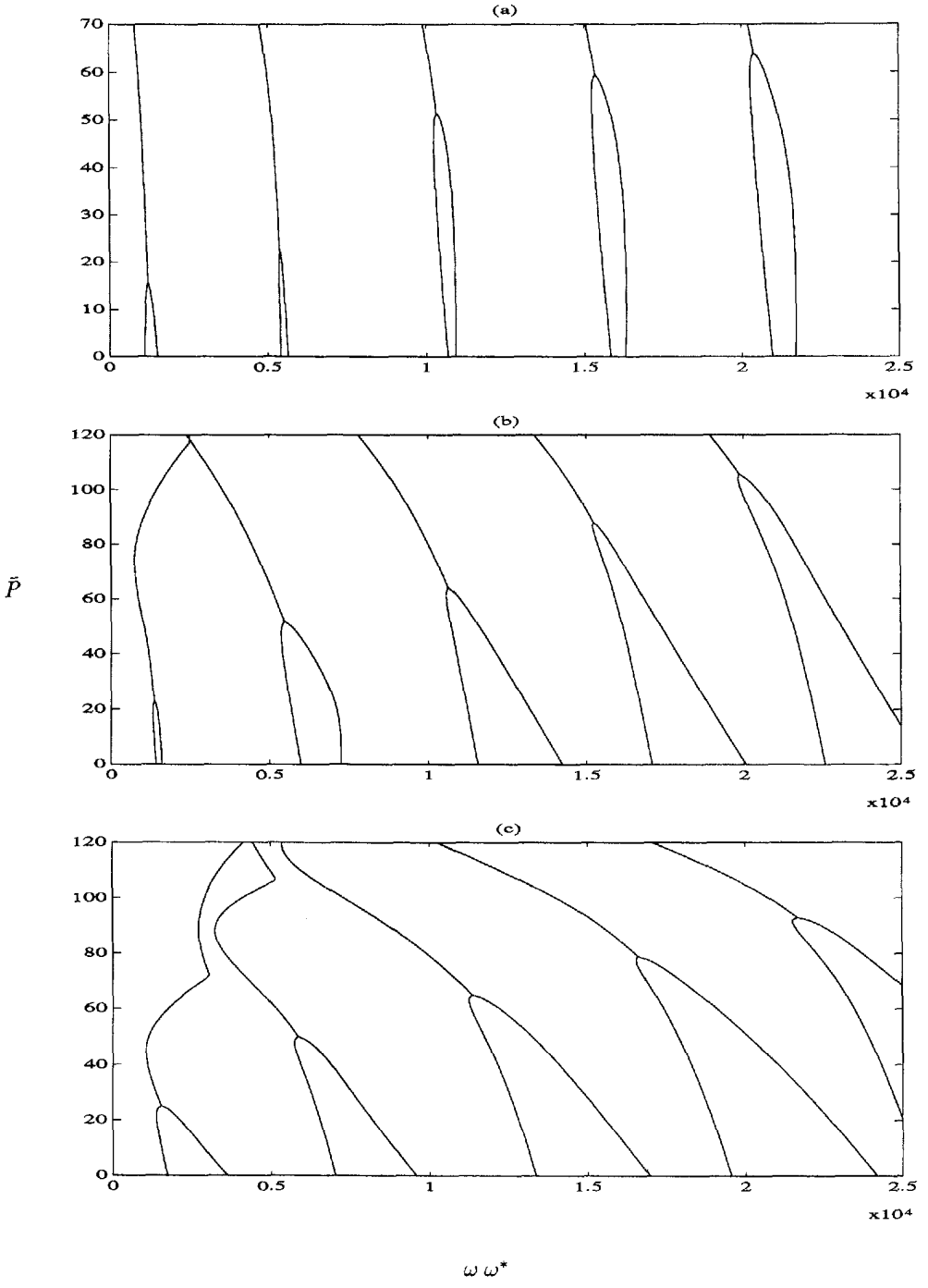

Fig. 8. The load–frequency curves for a tapered cantilever rod ($\alpha_h = 0$) subjected to a follower force on an elastic foundation with $\bar{k}$ varying between 1000 and 20,000. (a) $\alpha_h = 0.05$; (b) $\alpha_h = 0.2$; (c) $\alpha_h = 0.5$.

The load–frequency diagrams for a tapered beam resting on a viscoelastic foundation with c in the reasonable range between 0 and 0.2 are found to be the same as the corresponding frequency diagrams for a tapered beam resting on an elastic foundation without damping. The presence of viscous damping in the elastic foundation therefore does not affect the critical flutter loads.

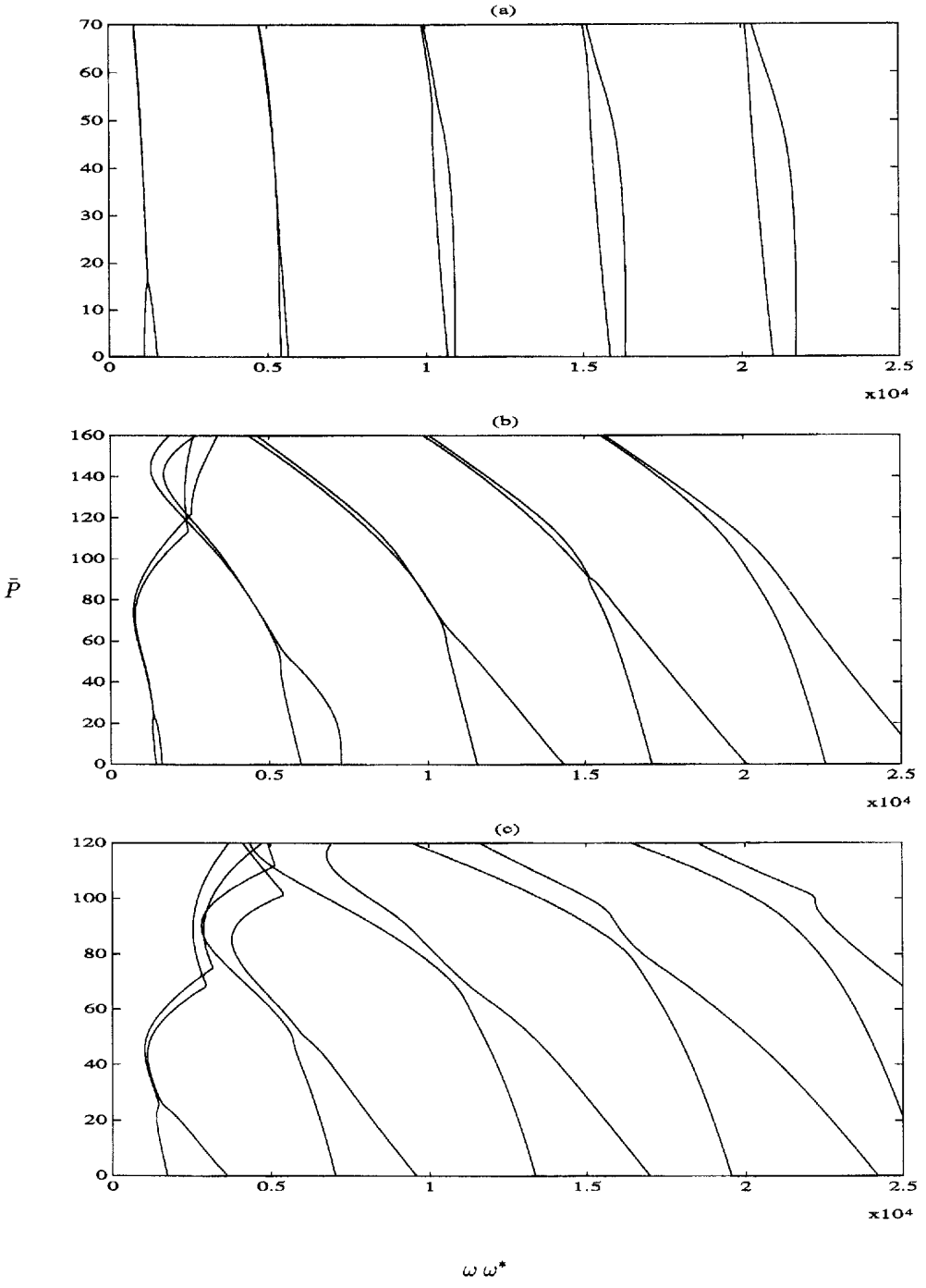

Fig. 9. The load–frequency curves for a tapered cantilever rod ($\alpha_h = 0$) subjected to a follower force on an elastic foundation with $\bar{k}$ varying between 1000 and 20,000; $\eta = 0.001$. (a) $\alpha_h = 0.05$; (b) $\alpha_h = 0.2$; (c) $\alpha_h = 0.5$.

4. CONCLUSION

For a beam of uniform cross-section resting on an elastic foundation subjected to a tip-concentrated follower force, the numerical studies show that:

1. The critical flutter loads are insensitive to variation in the modulus of the elastic foundation in the presence or absence of damping.

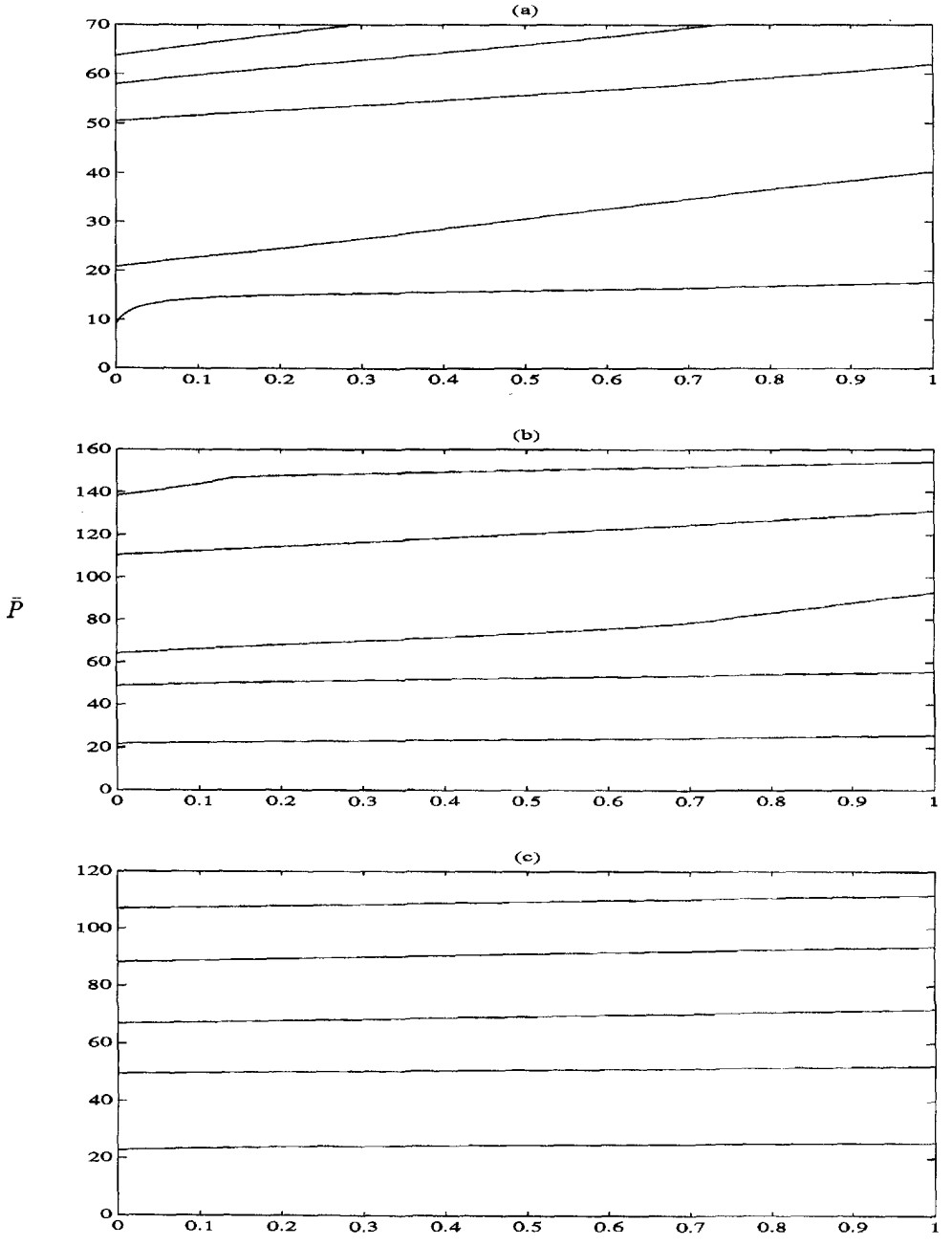

Fig. 10. The real part of ω for the load–frequency curves presented in Fig. 9; $\eta = 0.001$. (a) $\alpha_h = 0.05$; (b) $\alpha_h = 0.2$; (c) $\alpha_h = 0.5$.

2. The critical flutter loads are insensitive to the presence of viscous damping.
3. The critical flutter loads are drastically reduced by the presence of small amounts of internal damping.

For a uniformly tapered beam resting on an elastic foundation subjected to a tip-concentrated follower force, the numerical studies show that:

1. The critical flutter loads are not affected by the presence of viscous damping in the elastic foundation.
2. The presence of small amounts of internal damping in the beam may reduce, increase, or may not affect the critical flutter load depending on the taper ratio as well as the modulus of the elastic foundation.

REFERENCES

Bolotin, V. V. (1964). *The Dynamic Stability of Elastic Systems*. Holden-Day, San Francisco.

Bolotin, V. V. (1965). *Nonconservative Problems of the Theory of Elastic Stability*. Pergamon Press, London.

Bolotin, V. V. and Zhinzher, N. I. (1969). Effects of damping on stability of elastic systems subjected to nonconservative forces. *Int. J. Solids Structures* **5,** 965–989.

De Rosa, M. A. and Franciosi, C. (1990). The influence of an intermediate support on the stability behavior of cantilever beams subjected to follower forces. *J. Sound Vibr.* **137,** 107–115.

Elishakoff, I. and Lottati, I. (1988). Divergence and flutter of nonconservative systems with intermediate supports. *Comput. Meth. Appl. Mech. Engng* **66,** 241–250.

Guran, A. and Rimrott, F. P. J. (1989). On the dynamic stability of an elastic rod under a slave tip loading. In *Vibration Analysis—Techniques and Applications*, DE-Vol. 18-4, pp. 225–228. ASME, New York.

Hauger, W. and Vetter, K. (1976). Influence of an elastic foundation on the stability of a tangentially loaded column. *J. Sound Vibr.* **47,** 296–299.

Herrmann, G. and Jong, I. C. (1965). On the destabilizing effect of damping in nonconservative elastic systems. *J. Appl. Mech.* **32,** 592.

Herrmann, G. and Jong, I. C. (1966). On nonconservative stability problems of elastic systems with slight damping. *J. Appl. Mech.* **33,** 125.

Kounadis, A. N. (1983). The existence of regions of divergence instability for nonconservative systems under follower forces. *Int. J. Solids Structures* **19,** 725–733.

Lee, H. P. (1994). Divergence and flutter of a cantilever rod with an intermediate spring support. *Int. J. Solids Structures* (To appear).

Lee, S. Y. and Yang, C. C. (1994). Non-conservative instability of non-uniform beams resting on an elastic foundation. *J. Sound Vibr.* **169,** 433–444.

Lee, S. Y., Kuo, Y. H. and Lin, F. Y. (1992). Stability of a Timoshenko beam resting on a Winkler elastic foundation. *J. Sound Vibr.* **153,** 193–202.

Leipholz, H. (1980). *Stability of Elastic Systems*. Sijthoff and Noordhoff, The Netherlands.

Levinson, M. (1966). Application of the Galerkin and Ritz methods to nonconservative problems of elastic stability. *ZAMP* **17,** 431–442.

Nageswara Rao, B. and Venkateswara Rao, G. (1987). Applicability of static or dynamic criterion on the stability of a cantilever column under a tip concentrated subtangential follower force. *J. Sound Vibr.* **118,** 197–200.

Nageswara Rao, B. and Venkateswara Rao, G. (1988). Stability of a cantilever column under a tip-concentrated subtangential follower force with the value of sub-tangential parameter close to or equal to 1/2. *J. Sound Vibr.* **121,** 181–188.

Nageswara Rao, B. and Venkateswara Rao, G. (1990). Stability of a cantilever column under a tip-concentrated subtangential follower force with damping. *J. Sound Vibr.* **138,** 341–344.

Nemat-Nasser, S. (1967). On the stability of the equilibrium of nonconservative continuous systems with slight damping. *J. Appl. Mech.* **34,** 344–348.

Ryu, B. J. and Sugiyama, Y. (1994). Dynamic stability of cantilevered Timoshenko columns subjected to a rocket thrust. *Comput. Structures* **51,** 331–335.

Smith, T. E. and Herrmann, G. (1972). Stability of a beam on an elastic foundation subjected to a follower force. *J. Appl. Mech.* **39,** 628–629.

Sundararajan, C. (1974). Stability of columns of elastic foundation subjected to conservative and nonconservative forces. *J. Sound Vibr.* **37,** 79–85.

Venkateswara Rao, G. and Kanaka Raju, K. (1982). Stability of tapered cantilever columns with an elastic foundation subjected to a concentrated follower force at the free end. *J. Sound Vibr.* **81,** 147–151.

Ziegler, H. (1968). *Principles of Structural Stability*. Blaisdell Publishing Company, Toronto.